Available online at www.sciencedirect.com
ScienceDirect
Journal of the European Ceramic Society 29 (2009) 3265–3271
www.elsevier.com/locate/jeurceramsoc

Thick-film NTC thermistors and LTCC materials: The dependence of the electrical and microstructural characteristics on the firing temperature

Marko Hrovat [a,*], Darko Belavič [b], Jaroslaw Kita [c], Janez Holc [a], Jena Cilenšek [a], Silvo Drnovšek [a]

[a] *Jožef Stefan Institute, Jamova 39, 1000 Ljubljana, Slovenia*
[b] *HIPOT-R&D, d.o.o., Trubarjeva 7, 8310 Sentjernej, Slovenia*
[c] *University of Bayreuth, Universitätsstrasse 30, 95440 Bayreuth, Germany*

Received 30 January 2009; received in revised form 8 May 2009; accepted 13 May 2009
Available online 11 June 2009

Abstract

The electrical and microstructural characteristics of 1 kΩ/sq. thick-film NTC thermistors (4993, EMCA Remex) fired either on LTCC (low-temperature cofired ceramic) substrates or buried within LTCC structures were evaluated. The thermistors were fired at different temperatures to study the influence of firing temperature on the electrical characteristics. The results were compared with the characteristics obtained on alumina substrates. The sheet resistivities were higher than the resistivities of thick-film thermistors on alumina substrates. The increase of the sheet resistivities was attributed to the diffusion of the glass phase from the rather glassy LTCC substrates into the NTC thermistors. This was confirmed by EDS analyses. However, the increase in the resistivity was linked to an increase of the beta factors. Therefore, the results show that the evaluated NTC thermistors on LTCC substrates can be used for temperature sensors in MCM-Cs as well as in MEMS LTCC structures. When the thermistors were buried in the LTCC substrates, the LTCC structures delaminated during firing, leading to high sheet resistivities and high noise indices. This delamination is attributed to the different sintering rates of the NTC and LTCC materials.

Keywords: Electron microscopy; X-ray methods; Electrical properties; Sensors

1. Introduction

The main required characteristics for thick-film resistor materials are a long-term stability, relatively narrow tolerances of the sheet resistivities after firing and a low temperature coefficient of resistivity (TCR). The TCRs for most resistors are under 100×10^{-6}/K. However, for temperature-sensing or temperature-compensating applications resistors with a large temperature dependence of resistivity – thermistors − are required.

The thermistors with negative TCRs have a large and non-linear temperature vs. resistivity dependence. Materials with large negative TCRs (NTC) are based on solid solutions of transition-metal oxides with the spinel structure (general formula AB_2O_4).

The dependence of the specific resistance ρ vs. temperature is described by[1]:

$$\rho = \rho_0 \times \exp\frac{B}{T} \quad (1)$$

where ρ_0 is the resistivity (Ω cm) at "infinite" temperature, T (K) is the temperature and B (K) is the thermistor constant (also called the beta factor or the coefficient of temperature sensitivity). The resistivity at "infinite" temperature is determined by the total number of octahedral "*B*" lattice sites in a spinel structure that can take part in the "hopping" conductivity process (there is no contribution to the overall conductivity if ions with different valences are on the tetrahedral "A" sites because the distance between the two "A" sites in a spinel lattice is too great for an electron "hopping" mechanism).[2,3] The B is defined as the ratio between the activation energy for electrical conduction and the Boltzman constant. Basically, it is a measure of the sensitivity − the "steepness" − of the resistivity vs. temperature curve. To calculate B from the measured resistances at different

* Corresponding author.
E-mail address: marko.hrovat@ijs.si (M. Hrovat).

0955-2219/$ – see front matter © 2009 Elsevier Ltd. All rights reserved.
doi:10.1016/j.jeurceramsoc.2009.05.019

temperatures Eq. (1) is normally re-written as

$$B = \ln \frac{R_1/R_2}{(1/T_1) - (1/T_2)} \quad (2)$$

where T (K) is the temperature (K) and R_1 and R_2 (Ω) are the resistances at T_1 and T_2, respectively.

Thermistor compositions are based mainly on Mn_3O_4, Co_3O_4 and NiO.[4–8] The values of the resistivities and the beta factors of NTC materials depend on the ratio of the oxides. The resistivities range from a few hundreds of Ω cm to a few tens of kΩ cm, the beta factors from 2500 to 4000 K and the temperature coefficients of expansion from 8.5×10^{-6}/K to 14.3×10^{-6}/K. A partial substitution of the iron oxide, alumina or silica on the "B" sites or copper oxide on the "A" sites increases or decreases the resistivities.[9–12] A few years ago Park[13] reported a significant increase in the beta factors when the NiO in the spinel structure is replaced by MgO.

Thick-film NTC thermistors consist of semi-conducting spinel and low-melting-point glass phases. The fired thickness is usually between 10 and 20 μm. The resistivities of the different spinel compositions are between a few hundreds of Ω cm and a few tens of kΩ cm. Due to the dimensions of the thick-film resistors the values of the sheet resistivities (Ω/sq.) are between two and three orders of magnitude higher than the resistivities (Ω cm) of the materials themselves. Therefore, materials for thick-film NTC resistors usually include some phase with a low specific resistance, generally RuO_2. This RuO_2 has a relatively low resistivity of 40×10^{-6} Ω cm,[14,15] and the addition of ruthenium oxide decreases the specific resistance, reduces the noise and improves the stability of the resistors.[4,16] However, due to the high, positive TCR of the RuO_2 it also decreases the beta factors. Jagtap et al.[17] recently reported beta factors close to 4000 K for thick films based on Mn–Co–Ni–O with the addition of 15 wt.% of RuO_2. However, the sheet resistivities were very high, around 20 MΩ/sq., which is far too high for practical applications.

Ceramic multi-chip modules (MCM-Cs) and micro-electromechanical systems (MEMS) are multilayer structures with a high density of interconnections. An additional advantage of the smaller size and higher density is the ability to integrate screen-printed resistors, or occasionally, capacitors and inductors. These components can be either screen printed on the surface or buried within the structures. Low-temperature co-fired ceramic (LTCC) materials, which are sintered at the low temperatures typically used for thick-film processing, i.e., around 850 °C, are widely used for the production of MCM-Cs and MEMS.[18] LTCCs are either based on crystallisable glass or a mixture of glass and ceramics.[19–23] Thick-film resistors with high TCRs could be useful as temperature sensors in MCM-Cs and MEMS.[24,25]

Like the majority of thick-film resistors the thick-film NTC thermistors are developed for firing on relatively inert alumina substrates. The compatibility and interactions with the rather glassy LTCC substrates, leading to changes in the electrical characteristics, need to be evaluated. The aim of this paper is to evaluate the characteristics of thick-film NTC 4993 (EMCA Remex, 1 kΩ/sq.) thermistors with nominal beta factors of 1200 K and an understanding of the development of the thick-film NTC thermistor's microstructural characteristics and electrical characteristics during the firing process. During a standard firing profile thick-film resistors are only a relatively short time (typically 10 min) at the highest temperature (typically 850 °C). The reactions between the constituents of the resistor material do not reach equilibrium, which means that the characteristics of the fired materials are, in a way, a compromise as a consequence of this frozen non-equilibrium.[26,27] Different firing conditions (temperature and time) will offer an insight into the evolution of these characteristics.

NTC 4993 thermistors fired either on the surface of LTCC tapes or buried within LTCC tapes were fired at temperatures from 850 to 950 °C, and also for a relatively long time (3 h) at 950 °C to allow the reactions to reach − or at least to come close to − equilibrium. The characteristics of NTC thermistors fired at the same temperatures on alumina substrates[28] are used as a reference.

2. Experimental

The LTCC substrates were made by laminating layers of 951 (Du Pont) LTCC tapes at 70 °C and at a pressure of 200 bar. For the surface NTC thermistors three layers were laminated. For the buried thermistors two layers were initially laminated. The conductive Ag/Pd tracks were then printed and dried on the laminated LTCC substrates. After this, the 4993 NTC thermistors were screen printed and dried. The upper tapes with the laser-cut openings (for the electrical measurements) were pressed into the two-layered structures and laminated again under the same conditions. The prepared samples were co-fired fired first for 1 h at 450 °C (burn-out of organics) and then fired at maximum temperatures of 850, 875 and 950 °C for 10 min, and at 950 °C for 3 h.

Cold (from −25 to 25 °C) and hot (from 25 to 125 °C) TCRs were calculated from resistivity measurements at −25, 25, and 125 °C. The current noise was measured in dB on 100-mW loaded resistors using the Quan Tech method (Quan Tech Model 315-C).

The dimensions of the resistor layers for the microstructural analysis and the X-ray diffraction (XRD) analysis were 12.5 mm × 12.5 mm. For the microstructural investigation the samples were mounted in epoxy in a cross-sectional orientation and then cut and polished using standard metallographic techniques. A JEOL JSM 5800 scanning electron microscope (SEM) equipped with an energy-dispersive X-ray analyzer (EDS) was used for the overall microstructural and compositional analysis. Boron oxide, which is also present in the glass phase, cannot be detected in the EDS spectra because of the low relative boron weight fraction in the glass and the strong absorption of the boron K_α line during the EDS analysis of the glass matrix. Dried thermistors (150 °C) and fired thermistors were analysed by X-ray diffraction (XRD) analysis with a Philips PW 1710 X-ray diffractometer using Cu Kα radiation.

For the sintering studies of the 951 LTCC and 4993 NTC materials the organic phases of the LTCC tapes and of the NTC paste was dissolved in acetone. The obtained powders were

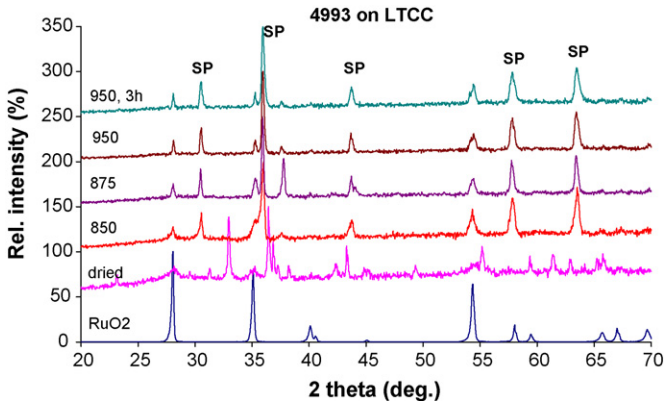

Fig. 1. X-ray diffraction spectra of the NTC 4993 thermistors dried at 150 °C and fired at different temperatures on LTCC substrates. The spectrum of ruthenate, denoted "RuO_2", is included. The peaks of spinel phase are denoted "SP".

pressed into pellets with a diameter of 6 mm and a height of 3 mm. The dimensional changes were measured in a heating-stage microscope. The heating rate was 10 K/min

3. Results and discussion

The X-ray diffraction spectra of the NTC 4993 thermistors dried at 150 °C, and fired for 10 min at 850, 875, and 950 °C, and 3 h at 950 °C on LTCC substrates are shown in Fig. 1. The spectrum of RuO_2, denoted "RuO_2", is included in the graph. The peaks of the spinel phase are denoted "SP". In the spectrum of the dried thermistors the peaks of the spinel phase are not present. After firing at 850 °C, as well as at higher temperatures, it is mainly the peaks of the spinel phase and of the ruthenium oxide that are observed. The X-ray analysis indicates that the semi-conducting spinel phase forms during firing and confirms the results presented in Ref. 28, where the formation of the spinel phase was detected between 500 and 700 °C. The spectra of the NTC thermistors fired on alumina and LTCC substrates for 10 min at 850 °C and for 3 h at 950 °C are compared in Fig. 2. The spectra of the NTC thermistors, fired on alumina and LTCC substrates, are nearly the same, regardless of the firing

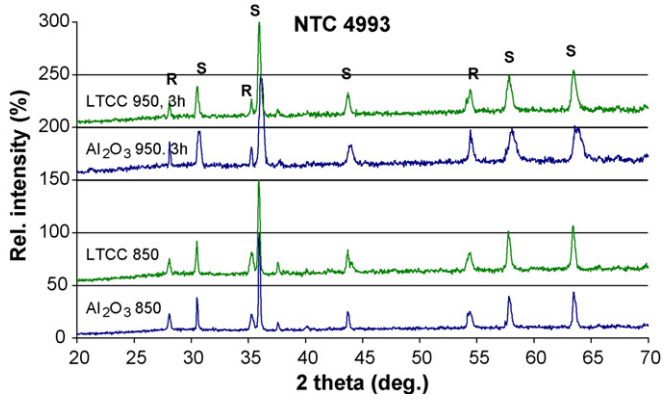

Fig. 2. X-ray spectra of NTC 4993 thermistors fired on alumina and on 951 LTCC substrates for 10 min at 850 °C and for 3 h at 950 °C. RuO_2 is denoted "R" and the spinel phase is denoted "S".

temperature, which indicates the compatibility of the thick-film NTC 4993 thermistors with the LTCC substrates.

Cross-sections of the NTC 4993 thermistors fired on LTCC substrates for 10 min at 850, 875 and 950 °C, and 3 h at 950 °C, are shown in Fig. 3a–d, respectively. The LTCC substrates are on the right. The LTCC material is composed of a glassy matrix (grey phase) and an alumina filler (dark phase). The microstructure of the NTC thermistor fired at 850 °C on an alumina substrate[28] is shown for comparison in Fig. 3e. The NTC thermistors fired at 850 °C on alumina and LTCC substrates are porous. However, the pores are smaller in the case of the thick films fired on LTCC substrates. And at higher firing temperatures the NTC films on LTCC substrates are less porous. The PbO-rich glass phase from the NTC film infiltrated the LTCC substrate and can be seen as a lighter layer at the interface between the NTC films and LTCC substrates. The depth of the diffusion from the NTC layer into the LTCC substrate was a little below 20 μm for a 10-min firing at 950 °C and over 40 μm for samples fired for 3 h at 950 °C.

The EDS analyses of the concentrations of elements (in at.%) and oxides (in mol%) in the NTC 4993 thermistors fired at 850 °C on the alumina and LTCC substrates are presented in Table 1. Noticeable is a higher concentration of silica in the NTC films fired on LTCC substrates, indicating the diffusion of the silica-rich glass from the LTCC into the NTC films during firing.

During the firing of the buried NTC thermistors the structures significantly delaminated, forming cavities between the upper and lower LTCC tapes. This naturally also resulted in the deformation of the LTCC tapes. The microstructure of the sample fired for 10 min at 850 °C is shown in Fig. 4. The light layers on the inner surfaces of the cavity are NTC films. The thickness of the buried NTC film is around half that of the thickness of the films on the LTCC, because the single layer separated into two layers on the bottom and the top of the cavity.

The cavities – or blisters – are formed due to the different shrinkage rates of the LTCC tapes and the thick-film NTC resistors during firing. The sintering curves of the LTCC and the NTC materials are shown in Fig. 5. The LTCC starts to sinter at around 650 °C, with the final shrinkage being 13% at 850 °C. The NTC material starts to sinter at a temperature around 500 °C, i.e., some 150 °C lower than the LTCC material. The maximum shrinkage was a little below 8%. Then the glass viscosity became low enough so that the sample pellet started to deform and slump down. Different shrinkage rates led to the de-lamination of the LTCC structures with buried NTC thermistors as the NTC films start to shrink at lower temperatures and "pull together" the upper and lower LTCC tapes.

However, note the "kink" in the NTC sintering curve. At 600 °C the pellet started to expand with the increasing temperature and then began to shrink again at around 750 °C. The reason for this (admittedly, this is beyond the scope of this paper) is the formation of the spinel phase. As reported by Hrovat et al.,[28] the XRD peaks of the spinel phase are not present in the dried NTC 4993 thick films, but appear at firing temperatures over 600 °C, indicating that the semi-conducting spinel phase forms during the firing. Spinels, at least the spinels present as func-

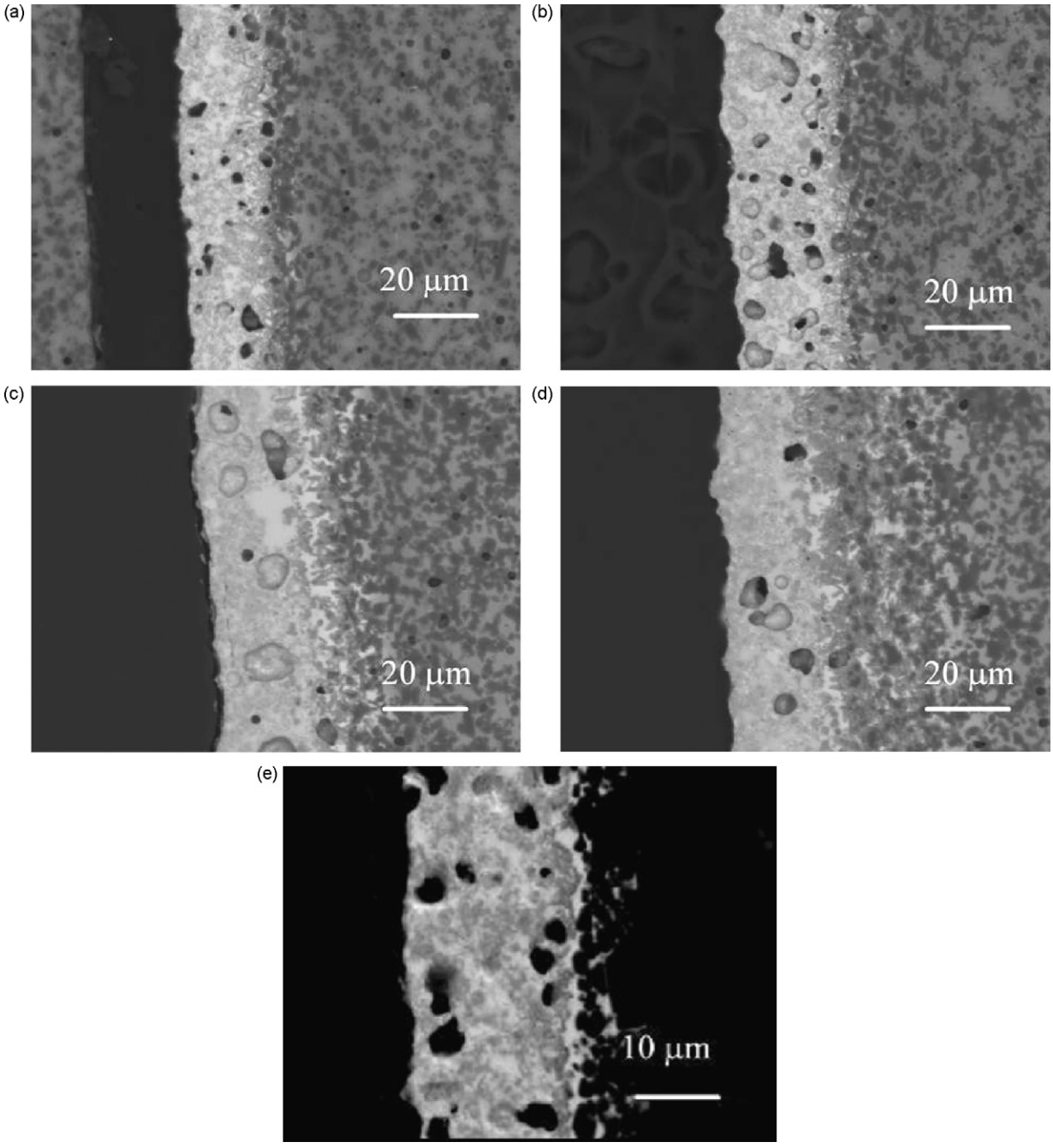

Fig. 3. (A) Cross-section of NTC 4993 thermistor fired at 850 °C on a 951 LTCC substrate. The LTCC substrate is on the right. Back-scattered electrons. (b) Cross-section of NTC 4993 thermistor fired at 875 °C on a 951 LTCC substrate. The LTCC substrate is on the right. Back-scattered electrons. (c) Cross-section of NTC 4993 thermistor fired at 950 °C on a 951 LTCC substrate. The LTCC substrate is on the right. Back-scattered electrons. (d) Cross-section of NTC 4993 thermistor fired for 3 h at 950 °C on a 951 LTCC substrate. The LTCC substrate is on the right. Back-scattered electrons. (e) Cross-section of NTC 4993 thermistor fired at 850 °C on alumina. The alumina substrate is on the right. Back-scattered electrons.[28]

tional phases in thick-film NTC thermistors, have larger cell volumes than the starting oxides. Let us take, just for an example, the reaction describing the formation of NiM_2O_4. Similar results can be calculated for $NiCo_2O_4$ spinels or solid solutions of manganese and cobalt spinels.

$$NiO + Mn_2O_3 \rightarrow NiMn_2O_4$$

The cell volumes, the number of unit cells per cell volume (Z) and the reduced volume – the volume of unit cells (the cell volume divided by Z) – are presented for NiO, Mn_2O_3 and $NiMn_2O_4$ in Table 2. If the sums of the unit volumes of NiO and Mn_2O_3 are compared with the unit volume of the spinel, the latter unit volume is around 5% larger.

The sheet resistivities, the cold (−25–25 °C) and hot (25–125 °C) TCRs, the beta factors and the noise indices of the 4993 NTC resistors on alumina,[28] on LTCC substrates and buried in LTCC substrates are presented in Table 3. The results are also graphically presented in Fig. 6, the logarithm of sheet

Table 1
The EDS analyses of the concentration of elements (in at.%) and oxides (in mol%) in the NTC 4993 thermistors fired at 850 °C on the alumina and LTCC substrates.

Element (at.%)	Al_2O_3 substrate	LTCC substrate	Oxide (mol%)	Al_2O_3 substrate	LTCC substrate
Al	7	6	$AlO_{1.5}$	17	15
Si	5	9	SiO_2	12	19
K	<1	<1	$KO_{0.5}$	<2	<2
Ca	<1	<1	CaO	<2	<2
Mn	10	11	MnO_x	24	23
Co	4	4	CoO_x	10	9
Ni	2	2	NiO	5	4
Cu	6	6	CuO	14	13
Ru	2	2	RuO_2	5	4
Pb	4	4	PbO	10	9
O	57	56			

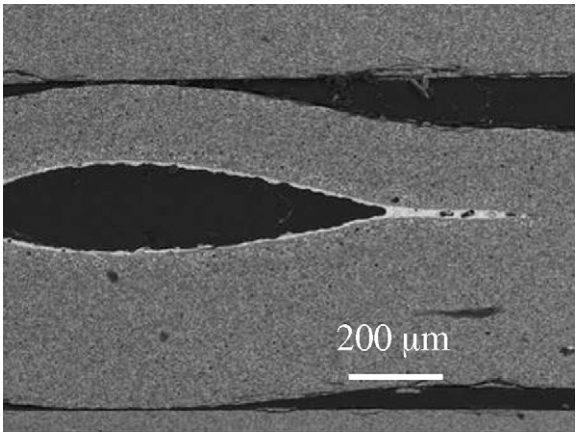

Fig. 4. Cross-section of NTC 4993 thermistor buried in the LTCC structure and fired at 850 °C. The structure delaminated.

Table 2
Cell volumes, number of unit cells per the cell volume (Z) and the reduced volume for NiO, Mn_2O_3 and $NiMn_2O_4$.

	Cell volume (A^3)	Z	Unit volume (A^3)
NiO	72.9	4	18.2
Mn_2O_3	838.6	16	52.4
$NiMn_2O_4$	592	8	74.1

resistivities, and 7, the noise indices, for the different firing conditions. The results for thermistors fired on alumina substrates[27] are added. The values for the buried thermistors are denoted "LTCC-b". The noise indices are shown in "dB" in Table 3 and in "μV/V" in Fig. 7. These two units are related by the simple equation:

$$\text{noise (dB)} = 20 \times \log \text{noise (}\mu\text{V/V)}$$

The noise indices for the thick-film NTC thermistors fired either on, or buried within, LTCC structures for a long time at the high temperature (3 h at 950 °C) were out of range of the QuanTech instrument, i.e., higher than 33 dB (44.7 μV/V). This is presumably due to the high resistivities of the NTC thermistors fired under these conditions.

The sheet resistivities are higher for the NTC thermistors fired either on, or buried within, LTCC ceramics than on alumina. At a "normal" firing temperature, i.e., 850 °C, the sheet resistivities of thick-film thermistors fired on alumina, on LTCC or buried within LTCC structures are around 0.6, 2.3 and 19 kΩ/sq., respectively. The sheet resistivities increase with higher firing temperatures. In the case of the NTC films on LTCC substrates this can be attributed to the diffusion of the (non-conducting) glass phase into the thermistor layers during firing. For buried thermistors a more probable reason is the delamination of the multilayered structures, as seen in Fig. 4. The beta factors

Table 3
Sheet resistivities, cold (−25–25 °C) and hot (25–125 °C) TCRs, beta factors and noise indices of the 4993 NTC resistors on alumina,[28] on LTCC substrates and buried in LTCC.

Substrate	T fir. (°C)	R sheet (kΩ/sq.)	Cold TCR ($\times 10^{-6}$/K)	Hot TCR ($\times 10^{-6}$/K)	B (K)	Noise (dB)	Noise (μV/V)
Al_2O_3[28]	850	0.55	−29930	−6530	1240	−12.9	0.23
	875	0.55	−20870	−6180	1150	−12.9	0.23
	950	1.5	−26550	−6700	1340	−20.4	0.10
	950, 3h	27	−47470	−7820	1820	−20.4	0.09
On LTCC	850	2.3	−41480	−7530	1660	3.0	1.41
	875	2.3	−39840	−7460	1620	3.3	1.47
	950	1.9	−37270	−7310	1555	9.3	2.79
	950, 3 h	200	−88540	−8780	2500	–[a]	–[a]
Buried LTCC	850	19	−58440	−8180	2020	−9.5	0.34
	875	17	−55320	−8080	1960	−4.0	0.63
	950	48	−85970	−8140	2030	2.7	1.36
	950, 3 h	850	−126670	−9160	2945	–[a]	–[a]

[a] Very high noise—out of range.

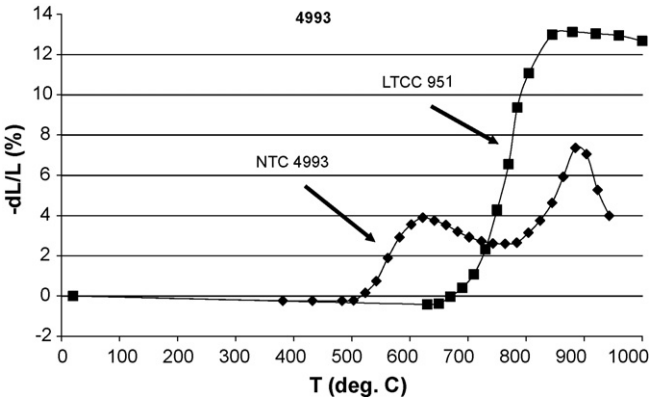

Fig. 5. Sintering curves of the LTCC 951 and NTC 4993 materials.

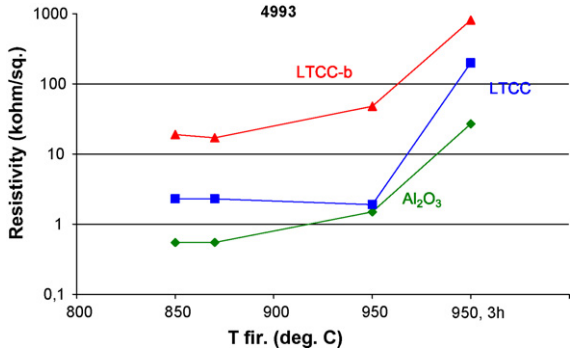

Fig. 6. The logarithm of sheet resistivities vs. firing temperatures for NTC 4993 thermistors fired either on, or buried within, LTCC structures. Results for thermistors fired on alumina substrates[28] are added. Values for buried thermistors are denoted "LTCC-b".

increase together with the sheet resistivities for higher firing temperatures.

The noise indices of the 4993 thermistors fired on alumina are relatively low, regardless of the firing conditions, and can be compared with the noise indices of the "ordinary" thick-film resistors with low TCRs and with the same nominal sheet resistivities, i.e., 1 kΩ/sq.[27] However, the noise of the thermistors fired either on, or buried inside, the LTCC substrates is higher and increases with higher firing temperatures. As mentioned before, it cannot be measured for the NTC/LTCC combinations fired for 3 h at 950 °C due to very high sheet resistivities.

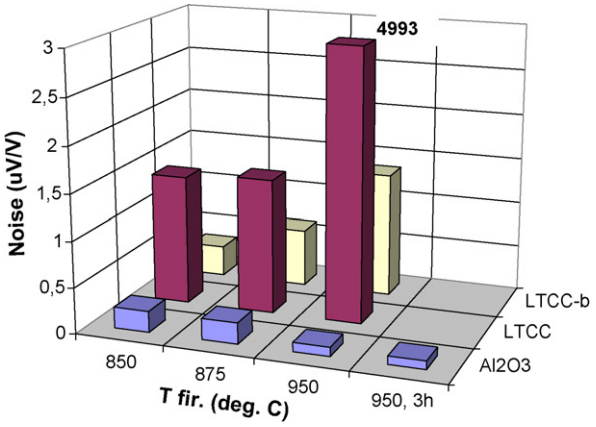

Fig. 7. The noise indices vs. firing temperatures for NTC 4993 thermistors co-fired either on, or buried within, LTCC structures. Results for thermistors fired on alumina substrates (27) are included. Values for buried thermistors are denoted "LTCC-b".

The results presented in this paper indicate that the investigated NTC thick-film thermistor (4993) can be used as a temperature sensor on LTCC ceramics if some higher noise indices are acceptable. The differences in the electrical characteristics of the NTC thermistors fired on the LTCC substrates compared with the results on the alumina substrates can be attributed to the interaction between the NTC films and the glassy LTCC substrates during firing. However, higher noise indices and the very high measured sheet resistivities of the buried thermitors are the consequence of the delamination crack within the LTCC structures.

4. Conclusions

Thick-film thermistors with high, negative TCRs were developed for firing on inert alumina substrates. Therefore, their compatibility with (rather glassy) LTCC substrates was evaluated. The NTC 4993 thermistors with a nominal sheet resistivity of 1 kΩ/sq. were printed and fired either on the surface of the LTCC substrates or buried within the LTCC structures. To evaluate the influence of the firing conditions the thermistors were fired at temperatures between 750 and 950 °C for 10 min, and also a rather long time (3 h) at 950 °C. The results showed that the buried NTC thermistors fired within the LTCC structures cannot be used for practical applications. During firing the LTCC structures delaminated due to the different shrinking rates of the NTC and LTCC materials leading to high sheet resistivities.

The sheet resistivities increase a little over 2 kΩ/sq. (less than 1 kΩ/sq. on alumina substrates) and the noise indices also increase up to 1.5 uV/V, but if this can be tolerated the NTC thermistors still have "useable" characteristics as temperature sensors because the beta factors are higher than for the same thick-film thermistors fired on alumina substrates.

References

1. Macklen, E. D., ed., *Thermistors*. Electrochemical Publications Ltd., Ayr, 1979, pp. 16–28.
2. Brabers, V. A. M. and Terhell, J. C., Electrical conductivity and cation valences in nickel manganite. *Phys. Status Solidi A*, 1982, **69**(1), 325–332.
3. Csete de Györgyfalva, G. D. C., Nolte, A. N. and Reaney, I. M., Correlation between microstructure and conductance in NTC thermistors produced from oxide powders. *J. Eur. Ceram. Soc.*, 1999, **19**(6-7), 857–860.
4. Martin de Vidales, J. L., Garcia-Chain, P., Rojas, R. M., Vila, E. and Garcia-Martinez, O., Preparation and characterisation of spinel-type Mn–Ni–Co–O negative temperature coefficient ceramic thermistors. *J. Mater. Sci.*, 1998, **33**(6), 1491–1496.
5. Huang, J., Hao, Y., Lin, H., Zhang, D., Song, J. and Zhou, D., Preparation and characteristics of the thermistor materials in the thick-film integrated temperature-humidity sensor. *Mater. Sci. Eng.*, 2003, **B99**(1–3), 523–526.
6. Jagtap, S., Rane, S., Mulik, U. and Amalnerkar, D., Thick film NTC thermistors for wide range of temperature sensing. *Microelectron. Int.*, 2007, **24**(2), 7–13.
7. Prudenziati, M., ed., *Thick Film Sensors*. Elsevier, Amsterdam, 1994, pp. 127–150.

8. Kanade, S. A. and Puri, V., Electrical properties if thick-film NTC thermistors composed of $Ni_{0.8}Co_{0.2}Mn_2O_4$ ceramic: effect of inorganic oxide binder. *Mater. Res. Bull.*, 2008, **43**(4), 819–824.
9. Martinez Sarrion, M. L. and Morales, M., Preparation and characterization of NZC thermistors based on $Fe_{2+y}Mn_{1-x-y}Ni_xO_4$. *J. Mater. Sci.*, 1995, **30**(10), 2610–2613.
10. Park, K. and Bang, D. J., Electrical properties of Ni–Mn–Co–(Fe) oxide thick-film NTC thermistors prepared by screen printing. *J. Mater. Sci.: Mater. Electron.*, 2003, **14**, 81–87.
11. Metz, D., Caffin, P., Legros, R. and Rousset, A., The preparation, characterization and electrical properties of copper manganite spinels, $Cu_xMn_{3-x}O_4$, $0<x<1$. *J. Mater. Sci.*, 1989, **24**(1), 83–87.
12. Metz, R., Electrical properties of NTC thermistors made of manganite ceramics of general spinel structure: $Mn_{3-x-y}M_xN_yO_4$ $0<x+y<1$; M and N being Ni, Co or Cu. Aging phenomenon study. *J. Mater. Sci.*, 2000, **35**(18), 4705–4711.
13. Park, K., Structural and electrical properties of $FeMg_{0.7}Cr_{0.6}Co_{0.7-x}Al_xO_4$ $(0<x<0.3)$ thick film NTC thermistors. *J. Eur. Ceram. Soc.*, 2006, **26**(6), 909–914.
14. van Loan, P. R., Conductive ternary oxides of ruthenium, and their use in thick film resistor glazes. *Ceram. Bull.*, 1972, **51**(3), 242, 231–233.
15. Pierce, J. W., Kuty, D. W. and Larry, J. R., The chemistry and stability of ruthenium based resistors. *Solid State Technol.*, 1982, **25**(10), 85–93.
16. Hao, Y. D., Chen, L. J., Lin, H., Zhou, D. X. and Gong, S. P., Research on NTC thermally sensitive powder materials for thick-film thermistors. *Sens. Actuators*, 1993, **A35**(3), 269–272.
17. Jagtap, S., Rane, S., Gosavi, S. and Amalnerkar, D., Preparation, characterisation and electrical properties of spinel-type enviroment friendly thick film NTC thermistors. *J. Eur. Ceram. Soc.*, 2008, **28**(13), 2501–2507.
18. Golonka, L. J., Dziedzic, A., Kita, J. and Zavada, T., LTCC in microelectronic application. *Informacije MIDEM*, 2002, **32**(4), 272–279.
19. Hoffman, L. C., Crystallizable dielectrics in multilayer structures for hybrid microcircuits: a review. *Adv. Ceram.*, 1989, **26**, 249–253.
20. Shapiro, A. A., Elwell, D. F., Imamura, P. and MeCartney, M. L., Structure–property relationships in low-temperature cofired ceramic. In *Proceedings of the 1994 International Symposium on Microelectronics ISHM-94*, 1994, pp. 306–311.
21. Jean, J.-H. and Chang, C.-R., Camber development during cofiring Ag-based low-dielectric-constant ceramic package. *J. Mater. Res.*, 1997, **12**(10), 2743–2750.
22. Ting, C.-J., Hsi, C.-S. and Lu, H.-J., Interactions between ruthenium-based resistors and cordierite-glass substrates in low temperature co-fired ceramics. *J. Am. Ceram. Soc.*, 2000, **83**(12), 23945–32953.
23. Jones, W. K., Liu, Y., Larsen, B., Wang, P. and Zampino, M., Chemical, structural and mechanical properties of the LTCC tapes. In *Proceedings of the 2000 International Symposium on Microelectronics IMAPS-2000*, 2002, pp. 669–674.
24. Zhong, J. and Bau, H. H., Thick film thermistors printed on LTCC tapes. *Am. Ceram. Soc. Bull.*, 2001, **80**(10), 39–42.
25. Birol, H., Maeder, T., Jacq, C. and Ryser, P., Investigaton of interactions between co-fired LTCC components. *J. Eur. Ceram. Soc.*, 2005, **25**(12), 2065–2069.
26. Morten, B., Masoero, A., Prudenziati, M. and Manfredini, T., Evolution of ruthenate-based thick film cermet resistors. *J. Phys. D: Appl. Phys.*, 1994, **27**(10), 2227–2235.
27. Hrovat, M., Benčan, A., Belavič, D., Holc, J. and Dražič, G., The influence of firing temperatures on the electrical and microstructural characteristics of thick film resistors for strain gauge applications. *Sens. Actuators*, 2003, **A103**, 341–352.
28. Hrovat, M., Belavič, D., Holc, J. and Cilenšek, J., The development of the microstructural and electrical characteristics on NTC thick-film thermistors during firing. *J. Mater. Sci.*, 2006, **41**(18), 5900–5906.